Theoretical Insights on the Electronic Properties of Eosin Y, an Organic Dye for Photovoltaic Applications

Sandrine Hazebroucq, Frédéric Labat, Daniel Lincot, and Carlo Adamo*

Laboratoire d'Electrochimie et de Chimie Analytique, CNRS-UMR 7575, Ecole Nationale Supérieure de Chimie de Paris, 11 rue Pierre et Marie Curie, 75231 Paris Cedex 05, France

Received: February 8, 2008; Revised Manuscript Received: April 16, 2008

A theoretical analysis, based on density functional theory, has been carried out on the electronic properties of eosin yellowish (2′,4′,5′,7′-tetrabromofluorescein), a dye used for photovoltaic applications. In particular different oxidation states of the bare molecule as well as its complexes with a Zn dication have been considered, with the aim to gain some insights on its electro- and photochemical behavior. The calculations have been carried out both in the gas phase and in solution, this last modeled by a continuum model. Besides the agreement with the experimental data, our results allow for a better interpretation of the spectroscopic properties of this dye and their tuning by interaction with the solvent or metal atom in aqueous solution.

1. Introduction

Eosin yellowish (2′,4′,5′,7′-tetrabromofluorescein, EYH_2) is a well-known organic dye, characterized by a large π conjugated system, allowing $\pi-\pi^*$ transitions at low energy, i.e., in the visible part of the spectrum. Furthermore, this acidic molecule has an affinity for basic proteins and, in vivo, it gives different colors to the cells or to the tissues, according to the pH of the medium. For such peculiar characteristics EYH_2 has been widely used as a dye in many biological and medical fields, such as cytology, histology, hematology.[1,2] In chemistry, it has been studied as a photocatalyst[3] or as the main component in the fabrication of holographic optical elements,[4] this latter application being related to its fluorescent properties.

More recently, eosin has attracted the attention of the electrochemists as one of the possible candidates as dye for application in molecular-based photovoltaic devices.[5–11] In fact, in dye-based solar cells, the dye absorbs the light (i.e., the incoming photons) and an excited electron is then injected into the semiconductor conduction band while the dye is regenerated in its native form by interaction with a redox pair (e.g., I^-/I_3^-). Working principles of such devices have been exposed in many articles and reviews.[12,13] The peculiar molecular properties of the dyes, and the possibilities of related technological applications, are directly related to (a) the energetic spectrum that determines the optical absorption and emission characteristics, (b) the efficiency in electron injection from the excited state to the semiconductor, and (c) a fast and efficient regeneration of the dye cation after the electron injection. In the most studied systems, the semiconductor is TiO_2 and the dye is based on Ru and Os polypyridyl complexes, such as $Ru(bpy)_2(NCS)_2$ or $Ru(bpy)_2(CN)_2$.[14–16] These systems have attracted much interest, because they achieve a high energy conversion (up to 10%) for a photovoltaic system based on organometallic molecules.[12]

In this context, eosin can be seen as a natural alternative to the more complex organometallic systems in such hybrid dye/semiconductor cells.[5] In fact, not only do the intrinsic properties of eosin (absorption, cost, etc.) make it a possible substitute of the organometallic derivatives but also very recently a one-step self-assembly process of EYH_2 with a metal oxide (ZnO) has been reported.[9] This last point is of particular relevance, because the preparation of hybrid materials for photovoltaic applications is not straightforward. In fact, semiconductor materials have to be produced, notably, by a heat treatment, and therefore only heat-resistant materials can be used for practical application in solar cells.[17] In the case of ZnO/EYH_2 assembly, instead, a one-step electrodeposition from aqueous solution, in appropriate conditions, is sufficient to synthesize a thin film with the required properties (stability, conductivity, sensitized photoelectrode).[9] Besides the synthesis advantages, this process, able to give epitaxial growth, is not expensive and would allow the production of cheaper solar cells.[10] The obtained dye-loaded ZnO films adsorb light in the visible wavelength range and, under illumination, electron−hole pairs are generated, producing photocurrent.[11] This coelectrodeposition gives rise to single crystalline hybrid grains, containing a large amount of dye molecules, whose structure is strictly related to the electrochemistry potential used.[6,10] The applied potentials are generally close to the redox potential of EY, thus indicating that the oxidized and reduced species have a specific effect on the electrodeposition and on the growth mechanism. Therefore in the ZnO/EYH_2 assembly, eosin plays a relevant role, not only as photoactive part (dye) but also as building block in the determination of the final structure of the hybrid material. In this context, a better understanding of EYH_2 redox properties and of the related photochemical behavior is mandatory to give detailed insights of the elementary steps in the self-assembly process and how this determines the overall photochromatic properties.

At the same time, a complete theoretical analysis could provide hints on some key points, like the nature of both the ground and the excited states involved in the absorption and/or photoemission and their tuning by environmental (e.g., interaction with semiconductor or solvent) effects, thus leading to a better tuning of the photochemical behavior.

Though the electronic characteristics of Ru and Os polypyridyl complexes have been analyzed in detail,[18–20] very little theoretical work is available on the eosin molecule and its derived ions. Up to now, the few investigations carried out on eosin or on related xanthene dyes have been performed using approximate theoretical approaches (i.e., semiempirical models).

* Corresponding author. E-mail: carlo-adamo@enscp.fr.

10.1021/jp8011624 CCC: $40.75
Published on Web 07/17/2008

Nevertheless, density functional theory (DFT) has been remarkably successful at providing a means to evaluate a variety of ground-state properties with an accuracy close to that of post Hartree−Fock (HF) methods.[22,23] More recently, it has been shown that the time dependent DFT approach (TDDFT) offers a rigorous route to the evaluation of vertical electronic excitation spectra.[24–26] Several tests have shown that approaches including hybrid HF/DFT methods provide reliable results for low excitation energies.[27–30] Furthermore, we have recently introduced the so-called PBE0 model, a hybrid HF/DFT approach based on the Perdew−Burke−Erzenrhof (PBE) functional.[31,32] This approach overcomes many of the problems encountered with standard functionals, providing accurate excitation energies to both valence and Rydberg states of neutrals as well as of open-shell molecules.[33,34] At the same time, it provides accurate solvent shifts on the absorption spectra, when coupled with appropriate solvent models.[17,35,36]

This paper is aimed at gaining some insights into the physical chemistry and more specifically the electronic properties of the EYH_2 and related complexes with zinc, using this theoretical tool. The ground-state properties of these species in their native, reduced and oxidized forms, as well as their electronic absorption spectra have be examined, to rationalize experimental results of previous spectroelectrochemical study. Furthermore, our study allowed investigating the nature of the excited states of the different species and the bonding mechanism with the metal cation. This latter part of the study could give some insight on the more general problem of the surface−dye interaction in hybrid systems.[7,8]

2. Computational Details

All DFT calculations were carried out with a development version of the Gaussian code,[37] using a hybrid model referred to as PBE0.[32] This approach is obtained by casting the PBE exchange and correlation functionals[31] in a hybrid HF/DFT scheme, where the HF exchange ratio (1/4) is fixed a priori.[38]

All systems have been fully optimized in the gas phase, and in some cases in solvent, using the 6-31+G(d) basis set,[39] which provides, at the DFT level, converged geometrical parameters.[40] When not differently specified, the structural optimization were performed without symmetry constraints and using standard thresholds (i.e., residual forces less than 10^{-5} au). All the stationary points found were characterized by subsequent frequency calculations.

Absorption spectra were computed as vertical excitations from the corresponding energy minima using the TDDFT approach as implemented in Gaussian,[26] using the same basis set. It has recently showed that this basis set provides valence electronic transitions with a good accuracy.[34] All calculations for the doublet states (reduced and oxidized species) were performed within a spin-unrestricted formalism and spin contamination, monitored by the expectation value of S^2, was found to be negligible ($0.75 \leq \langle S^2 \rangle \leq 0.77$).

Solvent effects were evaluated using the polarizable continuum model (PCM).[41] In particular, optimized structures and solvation energies have been computed by a cavity model, namely, the united atoms topological model (UATM),[42] coupled with the conductor-like polarizable continuum model (CPCM).[43] Solvent shifts of excitation bands were evaluated by a recent nonequilibrium implementation of the polarizable continuum model (in its CPCM version).[44]

3. Results and Discussion

Eosin Y (Figure 1) belongs to the family of the xanthene dyes, and it can act either as an oxidizing or a reducing agent.

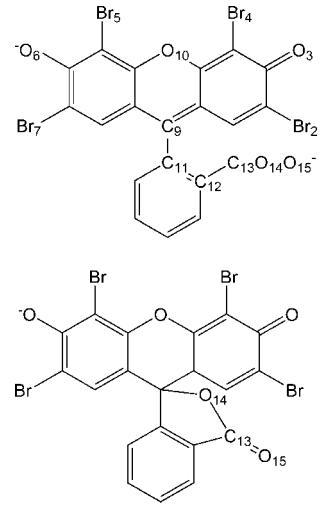

Figure 1. Sketches and atom labeling of the eosin Y dianion in its normal (quinoidal, up) and tautomeric (lactone, down) forms.

TABLE 1: Selected Geometrical Parameters (Å and deg) of the Bare and Zn-Complexed Eosin in Different Oxidation States[a]

	EY	EY (lactone form)	EY^-	EY^+	ZnEY	$ZnEY^-$
$O_{15}C_9$	2.52	1.61	2.92	1.53	2.75	2.92
$O_{15}C_{13}$	1.26	1.33	1.25	1.36	1.28	1.28
$O_{14}C_{13}$	1.25	1.22	1.27	1.21	1.28	1.28
$O_{15}Zn$					2.02	2.01
$O_{14}Zn$					2.03	2.05
$O_{15}C_{13}O_{14}$	130.1	125.1	129.0	123.9	119.4	119.3
τ^b	−3.7	−13.6	−1.2	−25.0	−0.9	−1.1
$C_{13}C_{12}C_{11}C_9$	0.0	0.0	6.9	0.0	1.8	1.2
$O_{15}C_{13}C_{12}C_{11}$	0.0	0.0	1.6	0.0	13.0	3.6

[a] See Figure 1 for atom labeling. [b] τ is the torsion angle of the middle-cycle of the anthracene group.

Its electrochemical behavior has been well characterized,[45] as well as its spectroscopic properties.[46–48] In particular, the absorption spectra of EYH_2 shows a strong pH dependency due to the protonation of the oxygen atoms or of the carboxyl group.[3] At the same time, the EYH_2 is subject to a tautomeric equilibrium between the quinoidal and lactone form, strongly affected by pH.[49] Nevertheless, because the pK_a value in water is 4.95[50] and the ZnO/EYH_2 hybrid films are prepared at a local pH of 10.5,[9] we will limit our attention to the deprotonated species. To this end we have considered the EY in its native form, the dianion (hereafter EY), as well as its reduced (trianion, EY^-) and oxidized (monoanion EY^+) derivatives. Two complexes with zinc, the neutral (ZnEY) and the reduced ($ZnEY^-$) ones will be also discussed.

3.1. Eosin and Its Redox Species. Let us start from the dianion form of EY, whose selected geometrical parameters of the optimized structure are reported in Table 1 and the atom labeling is in Figure 1. In its most stable conformation the molecule has an overall C_s symmetry, the benzoate ring being perpendicular to the xanthene moiety. This overall geometrical rearrangement corresponds to a geometrical and electronic decoupling of the carboxyl group from the chromophore (xanthene group). Indeed, this latter group is not perfectly planar, because it is about 4° out of a perfect planarity (referred as angle τ in the table 1).

In Figure 2 is reported the corresponding infrared (IR) spectrum for the region 2000−800 cm^{-1}. This spectrum, as well as all the others reported, has been obtained by associating a single Lorenzian function to each computed harmonic frequency,

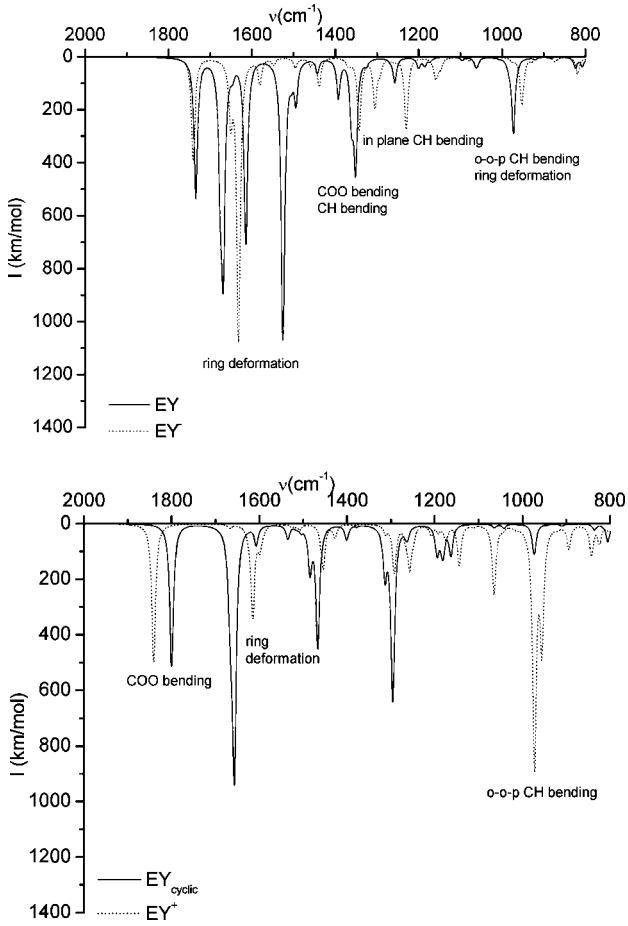

Figure 2. Theoretical IR spectra for eosin in the native/reduced forms (up) and cyclized/oxidized (down) forms. The spectra are reproduced by associating a single Lorentzian function with each computed wavenumber, with a half-height width of 10 cm^{-1}.

TABLE 2: Mulliken Atomic Charges (in |e⁻|) of Bare and Zn-Complexed Eosin in Different Oxidation States[a]

	EY	EY (lactone form)	EY^-	EY^+	ZnEY	$ZnEY^-$
Br_2	−0.21	−0.25	−0.29	−0.15	−0.07	−0.17
O_3	−0.58	−0.62	−0.66	−0.52	−0.47	−0.54
Br_4	−0.17	−0.19	−0.24	−0.10	−0.04	−0.13
O_{10}	−0.54	−0.55	−0.56	−0.54	−0.53	−0.53
Br_5	−0.17	−0.19	−0.24	−0.10	−0.03	−0.13
O_{15}	−0.59	−0.49	−0.60	−0.48	−0.59	−0.59
O_{14}	−0.61	−0.54	−0.66	−0.49	−0.59	−0.61
C_9	0.09	0.04	0.03	0.07	−0.01	−0.01
Zn					0.61	0.48

[a] See Figure 1 for atom labeling.

with a half-height width of 10 cm^{-1}. Four different regions can be considered as the fingerprint of such a molecular species: ring deformations (1700−1500 cm^{-1}), carboxylate and CH bending (around 1350 cm^{-1}), in-plane CH bending (around 1250 cm^{-1}) and out-of-plane bending (around 900 cm^{-1}). In particular, the COO bending of the carboxyl group has been calculated at 1361 cm^{-1}, in good agreement with the experimental value (1356 cm^{-1}).[51]

More information on the electronic structure of EY can be obtained from the analysis of Mulliken atomic charges, reported in Table 2. As it appears from these values, the oxygen atoms bear a significant negative charge, about 3 times larger than that located on bromines (∼0.6 |e⁻| vs ∼0.2 |e⁻|). It is not surprising, therefore, that, in aqueous solution, oxygens can be

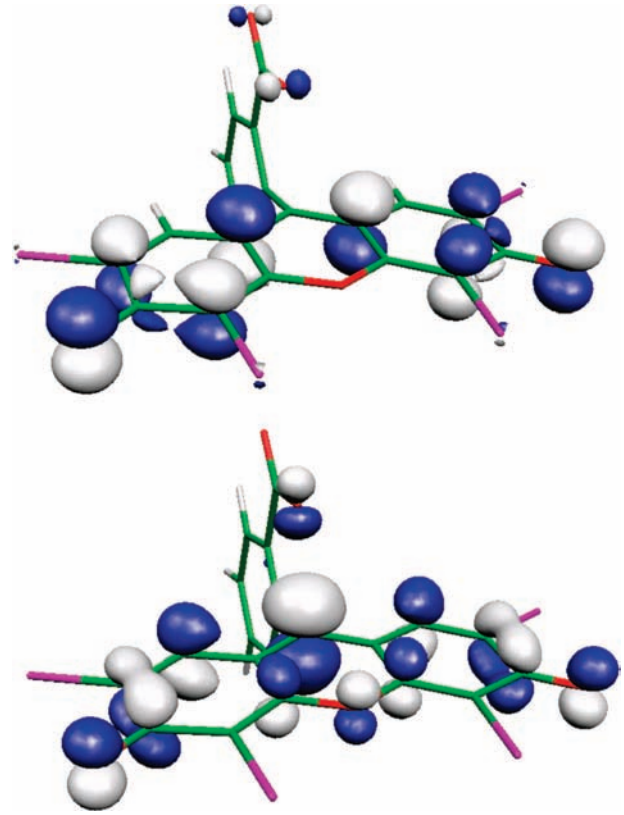

Figure 3. Representation of the highest occupied (up) and lowest unoccupied (down) molecular orbitals (HOMO and LUMO) of eosin Y dianion in its native form. The isosurface contour value is 0.05 au.

easily protonated and that, in thin films, they are coordinated to a counterion. At the same time, the carbon atoms linked to bromine atoms and the CH group are almost neutral whereas the carbon atoms adjacent to oxygen atoms all have a positive charge, between +0.3 and +0.4 |e⁻|. It is also noteworthy that the C_9 atom is slightly electron-deficient, its charge being +0.1 |e⁻|.

Complementary information can be derived from the analysis of the molecular orbitals. In Figure 3 are reported the highest occupied and lowest unoccupied molecular orbital (HOMO and LUMO, respectively) of EY. Both orbitals have a dominant π character, and they are mainly located on the xanthene part of the molecule, the main difference resting on the large contributions from the p orbitals of the C_9 and O_{15} atoms in the LUMO (see Figure 3b). This last orbital is occupied upon reduction of the native EY, and the corresponding electron affinities are computed to be 4.3 eV in the gas phase and 2.8 eV in aqueous solution. The extra electron is, indeed, spread over the whole molecule, as can been observed from the computed spin density map of Figure 4 (up) and from the Mülliken charges of Table 2. In particular, an increased negative charge is found on all the heteroatoms (Br and O), whereas the C_9 has a lower positive charge. A similar behavior has been found for all the atoms of the xanthene cycle not reported in the table. At the same time, the electronic population of the benzoate group is not modified by the reduction. These small modifications on the electronic distribution have a significant effect on the geometry. In fact, because the extra electron occupies the LUMO of the native form (figure 3), in which are present contributions from the π-system of the xanthene ring and from a p orbital of O_{15}, it simply "switches on" the repulsion between these two moieties and some geometrical distortions are induced to stabilize the

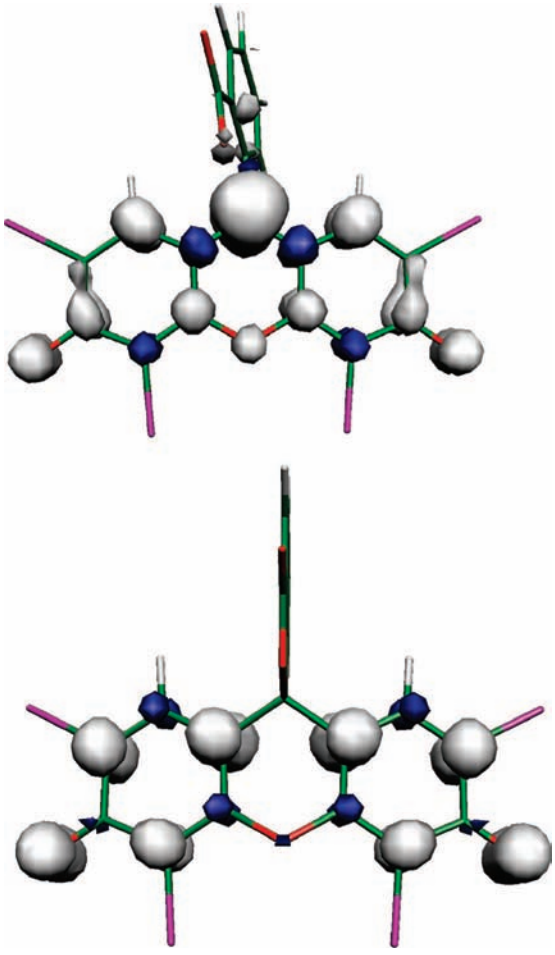

Figure 4. Computed spin density of the reduced (up) and oxidized (down) EY. The contour value is 0.003 au.

obtained radical. Significant variations affect the benzoate ring and, in particular, the carboxyl group upon reduction: the $O_{15}C_9$ distance is lengthened by 0.40 Å, and the $C_{13}C_{12}C_{11}C_9$ dihedral angle goes from zero to 6.9° (see table 1). All the other structural parameters are practically unaffected, especially as it concerns the aromatic rings. As expected, the IR spectrum is very sensitive to these electronic and structural modifications (see Figure 2). All the frequencies are shifted at lower energy with respect to the corresponding ones of the native forms, due to the antibonding character of the LUMO. As a consequence, the concerned bonds are weakened in the reduce form and their force constants are consequently smaller.

The reduced species of EY (EY^-) has been proposed to have a key role in the growth of zinc oxide in hybrid ZnO/EY materials,[52] characterized by a radial distribution of linear dye/oxide structures. The suggested hypothesis is based on a self-organization of EY during the codeposition, to form conducting chains with adjacent molecules. Because the excess electron is localized on the xanthene moiety, the maximization of the overlap between two adjacent molecules will lead to a ladder structure, well compatible with the advanced suggestions. Work is in progress on this point to elucidate the elementary steps of crystal formation.[53]

Finally, to have a better overview of the redox properties of the eosin, we have also analyzed the oxidized form (EY^+). This species is obtained by removing an electron from the HOMO of the native form (see Figure 3a), the calculated ionization potential being 0.9 eV in the gas phase and 5.0 eV in aqueous solution. The depletion of such an orbital, coupled with a strong electronic reorganization, has a dramatic effects on the geometrical rearrangement of EY^+, as can be seen from the data of Table 1. In particular, the largest change is the formation of a bond between the carboxyl group and the xanthene ring; that is, the benzoate group became a benzofuranolate (see Figure 1). The $O_{15}C_9$ distance is, therefore, shortened to 1.53 Å. This bond formation is coupled with a breaking of the conjugation in the xanthene plan, and the τ angle goes from −3.7 to −25.0°. The evident fingerprint in the IR spectrum of the new CO bond is represented by the strong shift of the COO scissoring, now centered at 1841 cm^{-1} (see Figure 2). At the same time, the frequencies corresponding at the out-of-plane motion of the CH strongly increase in intensity, thus showing the greater flexibility of EY^+ with respect to the native form. It must also be pointed out that the removal of one electron affects the charges of all the bromine atoms and, to a greater extent, of the oxygen atoms directly involved in the bond formations (O_{15} and O_{14}). The other oxygen atoms are, instead, not affected by the oxidation. The computed spin density map for the oxidized eosin (Figure 4, down) well illustrates the localization of the unpaired electron on the carbons and the carboxyl oxygens (O_3 and O_6) of the xanthene moiety. The presence of a lactone form for the oxidized form induced us to investigate the presence of the corresponding tautomer for the native form. The equilibrium of the quinoidal species with the lactone form has been investigated in details using electrochemical and spectroscopical techniques.[44,49,54,55] In particular, the quinoidal species of the native form of eosin has been estimated to be more stable of about 2.9 kcal/mol in nonpolar aprotic solvent.[49] The full optimization of the lactone form of EY leads to a stable tautomer that is only 3.8 kcal/mol higher in energy with respect to the most stable form in the gas phase. This difference is reduced to 3.4 kcal/mol in solution, thus leading to a nice agreement with the experimental data.[49] The geometrical parameters, reported in the third column of Table 1 are close to those obtained for the cyclic oxidized species, even if the xanthene ring is something flatter (τ −13.6° vs to −25.0°) and the bond $O_{15}C_9$ larger (1.61 vs 1.53 Å). This similarity between the two lactone forms of EY (native and oxidized) can be found also in the IR spectra of Figure 2b. Here the differences are related to a small shift of the COO bending and of a decreasing of intensities of the transitions related to the xanthene moiety.

3.2. Absorption Properties of EY. On the basis of the previous results, we have considered the absorption spectra of the EY in all the different oxidation states and both in the gas phase and in aqueous solution. To this end, the above optimized geometries have been used to compute vertical electronic transitions. The results are reported in Table 3. Starting from the native form, the results of the TDDFT computations show two intense transitions. The first band is centered at 433 nm: it is the most intense ($f = 0.6$) and can be assigned as a $\pi-\pi^*$ transition, corresponding to a one-electron excitation from the HOMO to the LUMO (see figure 3). The second one is an $n-\pi^*$ transition, centered at 403 nm, less intense ($f = 0.10$). Here the transition corresponds to HOMO−1 to LUMO excitation, the first orbital being mainly centered on the oxygen atoms of the carboxyl group. It is interesting to note that the HOMO/LUMO and (HOMO−1)/LUMO gaps corresponds to two transitions of 415 and 387 nm, respectively, thus showing their intrinsic one-electron nature. Both transitions are underestimated, of about 80 nm, with respect to the experimental data. In fact, the UV spectrum of the native dianion form of EY has been experimentally recorded and it shows one intense band at 516 nm, with a shoulder around 480 nm, both transitions being

TABLE 3: Wavelengths of the Main Vertical Transitions (λ, nm) and Corresponding Oscillators Strengths (f) for Eosin in Different Oxidation States and in the Complexes with Zinc[a]

	gas phase		solution			
molecule	λ	f	λ	f	assignment	exp
EY	433	0.64	444 (464)	0.87 (0.57)	$\pi-\pi^*$	516[b]
	403	0.10	347 (379)	0.14 (0.14)	n$-\pi^*$	~480[b]
EY^-	433	0.05	456	0.02	$\pi-\pi^*$	
	399	0.16	399	0.72	$\pi-\pi^*$	408[c]
EY^+	1960	0.13	2471	0.17	$\pi-\pi^*$	
	1097	0.01	414	0.04	$\pi-\pi^*$	
ZnEY	475	0.49	458	0.91	$\pi-\pi^*$	
	340	0.12	299	0.15	$\pi-\pi^*$	
$ZnEY^-$	603	0.13			$\pi-\pi^*$	
	583	0.11			$\pi-\pi^*$	

[a] In parentheses are reported the results obtained with the relaxed structure of EY in aqueous solution. [b] In aqueous solution at pH 7.4, ref 47, and in methanol, ref 48. [c] Reference 54.

recorded either in water (at pH 7.4) or in methanol.[47,48] This difference is slightly larger than expected for the level of theory used,[33,34] and it could be attributed to the lack of solvent effects. The results obtained with the CPCM model are reported in the fourth and fifth columns of Table 3. They show that solvent slightly red shifts the most intense band (+11 nm), which also increases in intensity, thus reaching the expected theoretical accuracy. At the same time a large solvent effect is observed, as expected, for the n$-\pi^*$ transition that is blue-shifted at 347 nm. An even larger effect is found when the molecular structure is relaxed in solution. In fact, the two bands are computed at 464 and 379 nm, respectively. Because the qualitative features of the spectra are already present in the calculations using the gas-phase geometries and due to the number of systems to be computed (some of them open-shell), in the following we will not consider structural relaxation in solution, but the spectra will be evaluated using the gas-phase geometries.

The reduction of the native form induces a breaking of the molecular symmetry, with a significant mixing of the orbitals of the xanthene and benzoate moieties. Nevertheless, small variations are observed in the transitions, with respect to the native form, the two main bands being centered at 433 and 399 nm. Both bands are significantly less intense with respect to those of EY, and they are both assigned as $\pi-\pi^*$ transitions. Therefore, it is not surprisingly that these bands are red-shifted by the interaction with the solvent, the variations being +23 and +1 nm, respectively. It is noteworthy that the intensity of the second band significantly increases in water. The most intense transition (399 nm) is in excellent agreement with the experiments (408 nm, ref 49).

More drastic is, instead, the effect of the oxidation, because the large electronic and structural rearrangements also affect the spectral properties. The spectrum of EY^+ is characterized by a plethora of weak transitions at very large wavelengths (low energies) corresponding to the excitations of β electrons from the manifold of occupied orbitals to the single occupied MO (SOMO). The most intense transition is center around 1960 nm (f=0.13). These last results are in agreement with experimental data which indicate that the oxidized form of EY is transparent in the UV−vis range.[9,56]

3.3. Complex with Zn. The next step in our study was to investigate the interaction of EY with one Zn dication. Because the electrodeposition takes place in reductive conditions,[9] we will not consider in the following the oxidized species and confine ourselves to the native (ZnEY) and reduced ($ZnEY^-$) complexes.

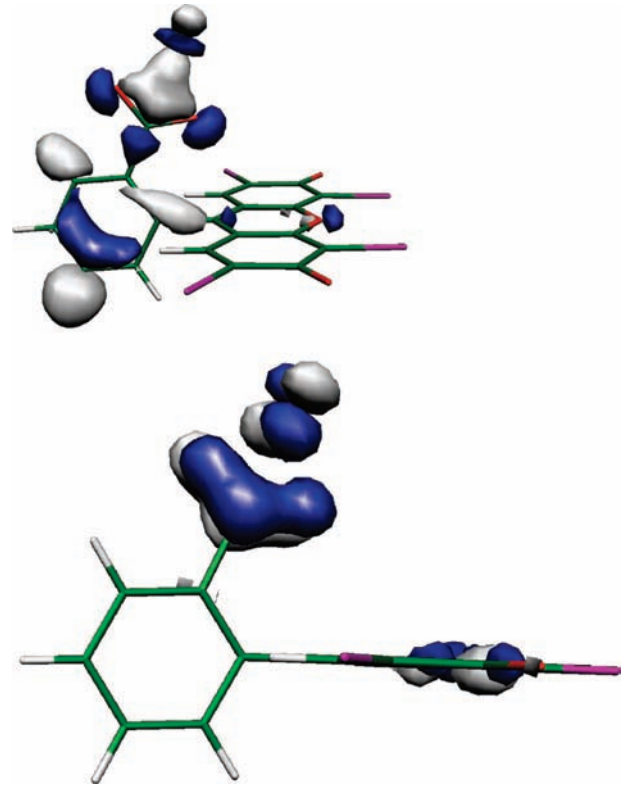

Figure 5. Representation of the orbitals corresponding to the zinc−eosin interaction. The isosurface contour value is 0.05 au.

As a first step, we investigated all the possible interaction of one Zn dication with all the negative atoms (O and Br) of EY. We found that the interaction with the carboxyl oxygens is, by far, the stronger, the interaction energies being 554 and 747 kcal/mol for the native and reduced species, respectively. These large energies arise, of course, from the interaction of a doubly charged metal cation (Zn) with the negative carboxyl group. The interaction has a significant charge transfer contribution as can be seen from the resulting Mulliken charges on the metal (see Table 2): +0.6 and +0.5 $|e^-|$ for ZnEY and $ZnEY^-$, respectively. It is interesting to note that in the complex, the carboxyl oxygen (O_{15} and O_{14}) bears the same charges as in the bare molecule, whereas the bromines are significantly depleted (−0.14 $|e^-|$) in going from the bare molecule to the complex. The orbitals responsible for this bonding interactions are reported in Figure 5. They well illustrate a σ (Figure 5, up) and π (Figure 5 down) interaction between the p orbitals of the carboxylate moiety and the d orbitals of the metal atom. These orbitals are quite low in energy, being about 8 eV more stable than the HOMO.

The interaction with the Zn cation induces small variations in the geometrical parameters of EY. In fact, a small increase of the carboxylate bonds, presumably due to electron back-donation from the metal to the ligand, is observed. This variations is accompanied by a significant (−11°) closure of the OCO angle and by a lengthening of the distance of the carboxyl group from the xanthene plan.

Significant variations are, instead, found in the electronic spectrum of eosin upon complexation. In fact, a new band appears at lower energies (475 nm) and it corresponds to an intense (f = 0.49) transition, clearly involving the metal atom. These theoretical results are in agreement with experimental data. In fact, a red shift of 43 nm is observed for the EY bands is 1:1 metal complexes,[56] very close to our theoretical data (42

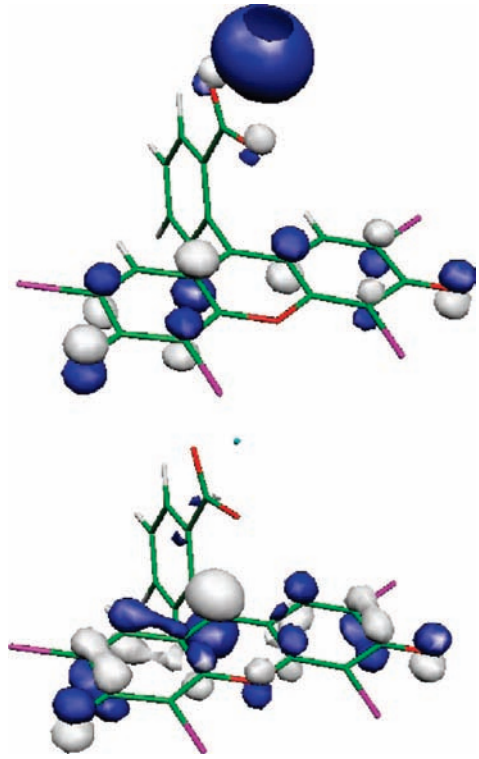

Figure 6. Representation of the highest occupied (up) and lowest unoccupied (down) molecular orbitals (HOMO and LUMO) of the complex of eosin Y with zinc. The isosurface contour value is 0.05 au.

nm). A smaller red shift (15 nm) has also been observed for other xanthene dyes adsorbed on titanium oxide particles.[7] The orbitals involved in this transition, the HOMO and the LUMO +1, are depicted in Figure 6. The first orbital is an antibonding orbital between the carboxyl group and the Zn atom, with a strong contribution of the 4s and 4p orbitals of the metal. The arrival orbital (LUMO+1) is a π^* orbital localized on the xanthene moiety.

A number of forbidden or very weak transitions has been found at lower wavelengths, but the first $\pi-\pi^*$ transition with a non-negligible oscillator strength is computed at 340 nm ($f =$ 0.12). When the solvent reaction field is taken into account, the two transitions are blue-shifted by about 17 and 41 nm, but both increase in intensity, the oscillator strengths in aqueous solution being 0.9 and 0.2, respectively.

These calculations on the electronic properties of EY and its complex with zinc could bring some light on the interpretation of the electronic signature of the bonding of eosin with a metallic or metallic oxide surface. In fact, this topic has been recently under debate.[7,8,57] In particular, three different modes of interaction have been envisaged on the basis of different interpretation of experimental spectroscopical data. The first mode, proposed by Ramakrishna and Ghosh, is based on the formation of a charge transfer complex between the xanthene dye and the oxide surface, involving the carboxyl group.[7] This hypothesis relies on the observation of a marked increase of the absorption of the dye in the presence of the oxide and of a red shift of absorption (and fluorescence) spectra.[7] Moser and co-workers[8] have discharged this possibility on the basis of semiempirical calculations. The main arguments they used rest on the electronic decoupling of the carboxyl group from the chromophoric (xanthene) part, as showed by the molecular orbital analysis of the bare EY. They have, then, proposed an alternative hypothesis based on H-bond anchoring of the dye with the hydroxylated oxide surface, suggesting a tripod configuration where the oxygen and the xanthene moiety (O_3 and O_6) are in direct contact with the oxide surface.[56] It must be noticed, anyway, that although this last suggestion could be valid for other molecules belonging to the xanthene family, the bulky bromine atoms sterically preclude such rearrangement.

In such a context, our DFT results clearly show the role played by the Zn and how its orbital contributions in the HOMO composition significantly influence the excitation behavior. Our calculations suggest that the red shift present in going from the bare EY to its Zn complex is not due to a polarization effects of the LUMO/HOMO orbital of the dye molecule generated by the metal atom. Rather the variation is related to the presence of a new band in the metal complex, arising from a strong orbital mixing involving metal orbitals. This band is, therefore, the signature of the strong electronic coupling between the metal atom and the carboxyl group. Even if the extrapolation from the interaction with one metal atom to the oxide surface is hazardous, our results seem to support the possibility of a charge transfer complex between the xanthene dye and the metals atoms of the oxide surface.

Finally the reduction of the ZnEY complex induces the apparition of two new bands, at 603 and 583 nm. None of these bands corresponds to an electron excitation from the metal atom, as expected. In fact, when an extra electron is added to the complex, a strong orbital mixing is observed, with a significant stabilization of the former LUMO +1 orbital, which become the LUMO of the reduced complex. At the same time the LUMO of the native species, characterized by a significant Zn contribution, is slightly destabilized. These transitions are assigned, therefore, as excitations of the unpaired electron of the SOMO, centered on the chromophore group, to the LUMO, this last having the main contribution from the benzoate ring. All the other computed bands present a negligible intensity (f < 0.03).

4. Conclusions

We have given a full description of the ground and excited states of eosin yellowish (2′,4′,5′,7′-tetrabromofluorescein) in its native, oxidized and reduced forms, using density functional theory. Our study focused on the spectral properties of the bare molecule and its complex with atomic Zn, in different oxidation states. The calculations have been carried out both in the gas phase and in solution, using a continuum model, to understand the environmental effects on the electronic properties. Besides the agreement with the experimental data, our results allow for a better interpretation of the spectroscopical properties of this dye and their tuning by interaction with the solvent or metal atom in solution. At the same, we have extrapolated our theoretical results to give some insight about the effects and the bonding mechanism with the oxide surface.

More generally, our results highlight the power of DFT approaches for the description of molecular dyes and their complexes, both in the ground and in the excited states. These theoretical approaches are especially helpful when the properties of the excited states can be only roughly derived from experimental data, thus providing clues for further improvement in the engineering of new photovoltaic materials.

Acknowledgment. C.A. is grateful to the French National Computer Center (IDRIS) for a generous grant of computer time (project 51703). We also thank the PPF ENSCP "Modélisation des Systèmes Complexes" for computer time.

References and Notes

(1) Bhattacharya, R.; Lakshmana Rao, P. V.; Vijayaraghavan, R. *Toxicol. Lett.* **2002**, *128*, 185.
(2) Wu, Y.; Li, B.; Gao, X. M. *Biotechnic Histochem.* **2002**, *77*, 291.
(3) Abe, R.; Hara, K.; Sayama, K.; Domen, K.; Arakawa, H. *J. Photochem. Photobiol. A* **2000**, *137*, 63.
(4) Manivannan, G.; Mailhot, G.; Bolte, M.; Lessard, R. A. *Pure Appl. Opt.* **1994**, *3*, 845.
(5) Moser, J.; Grätzel, M. *J. Am. Chem. Soc.* **1984**, *106*, 6557.
(6) Yoshida, T.; Terada, K.; Schlettwein, D.; Oekermann, T.; Sugiura, T.; Minoura, H. *Adv. Mater.* **2002**, *12*, 1214.
(7) Ramakrishna, G.; Ghosh, H. N. *J. Phys. Chem. B* **2001**, *105*, 7000.
(8) Pelet, S.; Grätzel, M.; Moser, J. E. *J. Phys. Chem. B* **2003**, *107*, 3215.
(9) Yoshida, T.; Pauporté, T.; Lincot, D.; Oekermann, T.; Minoura, H. *J. Electrochem. Soc.* **2003**, *150*, C608.
(10) Pauporté, T.; Yoshida, T.; Cortès, R.; Froment, M.; Lincot, D. *J. Phys. Chem. B* **2003**, *107*, 10077.
(11) Yoshida, T.; Iwaya, M.; Ando, H.; Oekermann, T.; Nonomura, K.; Schlettwein, D.; Wöhrle, D.; Minoura, H. *Chem. Commun.* **2004**, *400*.
(12) Hagfeldt, A.; Grätzel, M. *Acc. Chem. Res.* **2000**, *33*, 269, and references therein.
(13) Grätzel, M. *J. Photochem. Photobol. A* **2004**, *164*, 3.
(14) Sauvé, S.; Cass, M. E.; Coia, G.; Doig, S. J.; Lauermann, I.; Pomykal, K. E.; Lewis, N. S. *J. Phys. Chem. B* **2000**, *104*, 6821.
(15) Cecchet, F.; Gioacchini, A. M.; Marcaccio, M.; Paolucci, F.; Roffia, S.; Alebbi, M.; Bignozzi, C. A. *J. Phys. Chem. B* **2002**, *106*, 3926.
(16) Nazeeruddin, Md. K.; Pechy, P.; Renouard, T.; Zakeeruddin, S. M.; Humphry-Baker, R.; Comte, P.; Liska, P.; Cevey, L.; Costa, E.; Shklover, V.; Spiccia, L.; Deacon, G. B.; Bignozzi, C. A.; Gratzel, M. *J. Am. Chem. Soc.* **2001**, *123*, 1613.
(17) McEvoy, A. In *Practical Handbook of Solar Cells*; Markvart, T., Castaner, L., Eds.; Elsevier: Amsterdam, 2003; p 459.
(18) (a) Guillemoles, J.-F.; Joubert, L.; Barone, V.; Adamo, C. *J. Phys. Chem. A* **2002**, *106*, 11354. (b) Joubert, L.; Guillemoles, J.-F.; Adamo, C. *Chem. Phys. Lett.* **2003**, *371*, 378.
(19) (a) De Angelis, F.; Tilocca, A.; Selloni, A. *J. Am. Chem. Soc.* **2004**, *126*, 15024. (b) Nazeeruddin, M. K.; De Angelis, F.; Fantacci, S.; Selloni, A.; Viscardi, G.; Liska, P.; Ito, S.; Takeru, B.; Gratzel, M. *J. Am. Chem. Soc.* **2005**, *127*, 16835.
(20) Hoshiba, T.; Ida, T.; Mizuno, M.; Otsuka, T.; Takaoka, K.; Endo, K. *J. Mol. Struct.* **2002**, *602*, 381.
(21) Harryvan, D. H.; von Lubberhuizen, W. H.; Faassen, E.; Levine, Y. K.; Kothe, G. *Chem. Phys. Lett.* **1996**, *257*, 190.
(22) Koch, W.; Holthausen, M. C. *A Chemist's Guide to Density Functional Theory*; Wiley-VCH: Weinheim, Germany, 2000.
(23) Adamo, C.; di Matteo, A.; Barone, V. *Adv. Quantum Chem.* **1999**, *36*, 4.
(24) Runge, E.; Gross, E. K. U. *Phys. Rev. Lett.* **1996**, *76*, 1212.
(25) Bauernschmitt, R.; Ahlrichs, R. *Chem. Phys. Lett.* **1996**, *256*, 454.
(26) Stratmann, R. E.; Scuseria, G. E.; Frisch, M. J. *Chem. Phys.* **1998**, *109*, 8128.
(27) Tozer, D. J.; Handy, N. C. *J. Chem. Phys.* **1998**, *109*, 10180.
(28) Matsuzawa, N. N.; Ishitani, A.; Dixon, D. A.; Uda, T. *J. Phys. Chem. A* **2001**, *105*, 4953.
(29) Boulet, P.; Chermette, H.; Daul, C.; Gilardoni, F.; Rogemond, F.; Weber, J.; Zuber, G. *J. Phys. Chem. A* **2001**, *105*, 885.
(30) Jacquemin, D.; Preat, J.; Perpète, E. A. *Chem. Phys. Lett.* **2005**, *410*, 254.
(31) Perdew, J. P.; Burke, K.; Ernzerhof, M. *Phys. Rev. Lett.* **1996**, *77*, 3865; **1997**, *78*, 1396.
(32) Adamo, C.; Barone, V. *J. Chem. Phys.* **1999**, *110*, 6158.
(33) Adamo, C.; Barone, V.; Scuseria, G. E. *J. Chem. Phys.* **1999**, *111*, 2889. Adamo, C.; Barone, V. *Chem. Phys. Lett.* **2000**, *330*, 152.
(34) Ciofini, I.; Adamo, C. J. *Phys. Chem. A* **2007**, *111*, 5549.
(35) Adamo, C.; Barone, V. *Chem. Phys. Lett.* **1999**, *314*, 152.
(36) (a) Jacquemin, D.; Preat, J.; Charlot, M.; Wathelet, V.; André, J.-M.; Perpète, E. A. *J. Chem. Phys.* **2004**, *121*, 4389. (b) Jacquemin, D.; Wathelet; Perpete, E. A. *J. Phys. Chem. A* **2006**, *110*, 9145. (c) Perpete, E. A.; Wathelet, V.; Preat, J.; Lambert, C.; Jacquemin, D. *J. Chem. Theor. Comput.* **2006**, *2*, 434.
(37) Frisch, M. J.; Trucks, G. W.; Schlegel, H. B.; Scuseria, G. E.; Robb, M. A.; Cheeseman, J. R.; Montgomery, J. A., Jr.; Vreven, T.; Kudin, K. N.; Burant, J. C.; Millam, J. M.; Iyengar, S. S.; Tomasi, J.; Barone, V.; Mennucci, B.; Cossi, M.; Scalmani,G.; Rega, N.; Petersson, A.; Nakatsuji, H.; Hada, M.; Ehara, M.; Toyota, K. R.; Hasegawa, J.; Ishida, M.; Nakajima, T. ; Honda, Y.; Kitao, O.; Nakai, H.; Li, X.; Knox, J. E.; Hratchian, H. P.; Cross, J. B.; Adamo, C.; Jaramillo, J.; Gomperts, R.; Stratmann, R. E.; Cammi, R.; Pomelli, C.; Ochterski, J.; Ayala, P. Y.; Morokuma, K.; Hase, W. L.; Salvador, P.; Dannenberg, J. J.; Zakrzewski, V. G.; Dapprich, S.; Daniels, A. D.; Strain, M. C.; Farkas, O.; Malick, D. K.; Rabuck, A. D.; Raghavachari, K.; Foresman, J. B.; Ortiz, J. V.; Cui, Q.; Baboul, A. G.; Clifford, S.; Cioslowski, J.; Stefanov, B. B.; Liu, G.; Liashenko, A.; Piskorz, P.; Komaromi, I.; Martin, R. L.; Fox, D. J.; Keith, T.; Al-Laham, M. A. C.; Peng, Y.; Nanayakkara, A.; Challacombe, M.; Gill, P. M. W.; Johnson, B.; Chen, W.; Wong, M. W.; Gonzalez, C.; Pople, J. A. *Gaussian Development Version*, revision A.01; Gaussian Inc.:Pittsburgh, PA, 2005.
(38) Adamo, C.; Barone, V. *Chem. Phys. Lett.* **1997**, *274*, 242–250.
(39) Francl, M. M.; Petro, W. J.; Hehre, W. J.; Binkley, J. S.; Gordon, M.-H.; DeFree, D. J.; Pople, J. A. *J. Chem. Phys.* **1982**, *77*, 3654.
(40) KochW. Holthausen, M. C. *A Chemist's Guide to Density Functional Theory*; Wiley-VCH: Weinheim, Germany, 2000.
(41) Tomasi, J.; Persico, M. *Chem. Rev.* **1994**, *94*, 2027.
(42) Barone, V.; Cossi, M.; Tomasi, J. *J. Chem. Phys.* **1997**, *107*, 3210.
(43) Klamt, A.; Schüürmann, G. *J. Chem. Soc.,Perkin Trans. 2* **1993**, *799*.
(44) Cossi, M.; Barone, V. *J. Chem. Phys.* **2001**, *115*, 4708.
(45) (a) Issa, I. M.; Issa, R. M.; Ghoneim, M. M.; Temerk, Y. K. *Electrochim. Acta* **1973**, *18*, 265. (b) Bannerjee, N. R.; Negi, A. S. *Electrochim. Acta* **1973**, *18*, 335.
(46) Rohatapi, K.; Mukhophadhyali, A. *Photochem. Photobiol.* **1971**, *14*, 551.
(47) Birla, L.; Cristian, A. M.; Hillebrand, M. *Spectrochim. Acta A* **2004**, *6*, 551.
(48) Gratz, H.; Penzkofer, A. *J. Photochem. Photobiol. A* **1999**, *127*, 21.
(49) Mchedlov-Petrossyan, N. O.; Kukhtik, V. I.; Bezugliy, V. D. *J. Phys. Org. Chem.* **2003**, *16*, 380.
(50) Levitan, H. *Proc. Natl. Acad. Sci.* **1977**, *74*, 2914.
(51) Narayanan, V. A.; Stokes, D. L.; Vo-Dinh, T. *J. Raman Spectrosc.* **2005**, *415*, 25.
(52) (a) Lincot, D.; Yoshida, T.; Pauporté, T.; Goux, A.; Fromey, M.; Laval, J. Y.; Komatsu, D.; Ockerman, T. *19th European Photovoltaic Solar Energy Conference*, Paris, 7−11 June 2004. (b) Lincot, D.; Pauporté, T.; Goux, A.; Lain, V.; Yoshida, T. *207th ECS Meeting*,Quebec,15−20 May 2005.
(53) Lincot, D.; Adamo, C. manuscript in preparation.
(54) Fink, D. W.; Willis, C. R. *J. Chem. Phys.* **1970**, *53*, 4720.
(55) Goux, A.; Pauporté, T.; Lincot, D.; Dunsch, L. *Chem. Phys. Chem.* **2007**, *8*, 926.
(56) Rauf, M. A.; Ikram, M.; Ahmad, M. *Dyes Pigm.* **2002**, *52*, 183.
(57) Hilgendorff, M.; Sundström, V. *J. Phys. Chem. B* **1998**, *102*, 10505.

JP8011624